



Trade Science Inc.

Organic CHEMISTRY

*An Indian Journal**Full Paper*

OCAIJ, 8(9), 2012 [335-341]

Spectral, magnetic, corrosion studies and antimicrobial activity of O-Hydroxyacetophenone phenoxy acetylhydrazone (H₂OAPA)

Magdy M.Bekheit¹, Mohamed T.Gad Allah², Amira R.El-Shobaky^{2*}¹Chemistry Department, Faculty of Science, Mansoura University, (EGYPT)²Chemistry Department, Faculty of Science, Mansoura University, Damietta Branch, (EGYPT)

E-mail: aelshobaky@yahoo.com

Received: 16th January, 2012 ; Accepted: 8th February, 2012

ABSTRACT

Complexes of o-hydroxyacetophenone phenoxyacetylhydrazone (H₂OAPA) structure(I, II). with Co(II), Ni(II), Cu(II), Zn(II), Cd(II) and UO₂(IV) have been prepared and characterized on the basis of chemical analyses, molar conductivities measurements, spectral (IR, ¹H NMR, UV-Vis), and magnetic moment. IR and ¹H NMR spectral data show that (H₂OAPA) behaves as a neutral bidentate and mononegative or binate tridentate ligand. All the reported complexes are non-electrolytes and different stereo-chemistries are proposed for the Co(II), Ni(II) and Cu(II) complexes according to their magnetic and spectral measurements.

© 2012 Trade Science Inc. - INDIA

KEYWORDS

Hydrazone complexes;
NMR;
Corrosion;
Biological activity.

INTRODUCTION

Hydrazones have interesting ligation properties due to the presence of several coordination sites. Hydrazones and their metal complexes have attracted considerable attention due to their application in numerous industrial and biological fields^[1-3]. Hydrazones derivatives of o-Hydroxyacetophenone-have were reported^[4-14] with different metal salts to form new complexes which have been characterized by elemental analyses and molar conductance. We now report the syntheses, spectroscopic, magnetic, conductivity corrosion studies and antimicrobial activity of o-hydroxyacetophenone phenoxy acetylhydrazone (H₂OAPA).

EXPERIMENTAL

All chemicals used are BDH (British Drug LTD,

England) quality.

Synthesis of the ligand

O-hydroxyacetophenone pheno xyacetyl hydrazone (H₂OAPA) was prepared by heating o-hydroxyaceto phenone (13.6 ml, 0.1 mol) and phenoxyacetyl hydra zine(16.6 gm, 0.1 mol) in absolute ethanol (100 ml) for 0.5h. Upon cooling yellow crystals were separated. The product was filtered, washed, recrystllized from absolute ethanol and finally dried in a desiccator over fused CaCl₂, yield 25.7 gm, m.p 152 ° C.

Synthesis of metal chelates

The [Co(H₂OAPA)Cl₂(H₂O)₂] complex was prepared by adding an ethanolic solution (25 ml) of H₂OAPA (0.29 gm, 1 mmole) to the cobalt chloride (1 mmole) in the same solvent (50 ml). The [M(HOAPA)₂].2H₂O, (M= Cu(II) or Ni(II)) were pre-

Full Paper

pared by the same method using ethanolic solution (50 ml) of H₂OAPA (0.58 gm, 2 mmole) and (1 mmole) of the corresponding metal chloride. The reaction mixtures were heated under reflux for 0.5 h.

The complexes, [M(OAPA)(H₂O)₃], (M = Co(II), Ni(II), Cu(II) and Cd(II)), were prepared by adding ethanolic solution (25 ml) of H₂OAPA (0.29 gm, 1 mmole) to the corresponding metal acetate (1 mmole) in 25 ml ethanol or water. The [UO₂(HOAPA)₂] was prepared by the same method using (0.58 gm, 2 mmole) of H₂OAPA in 50 ml ethanol. The reaction mixtures were heated under reflux for 0.5 h.

Physical measurements

The metal and chloride contents were analyzed by standard method (Vogel, 1989). IR spectra were recorded on a Mattson 5000 FTIR Spectrometer as KBr discs; electronic spectra in dimethylformamide (DMF) were obtained using an UV2-100 Unicam UV-visible spectrometer. Magnetic moments at 25° C were determined using a Gouy balance. H¹ NMR spectra were recorded on Prucker Ac 400 Spectrometer at King Abd El-Aziz University. Molar conductivities in DMSO at 25° C were measured using a type CD6NGT Tacussel Conductivity Bridge.

Corrosion inhibition studies

The inhibitive action of the investigated ligand on the dissolution of aluminum in 0.5M hydrochloric acid, Aluminum was selected for this study due to its numerous industrial applications and consequently its corrosion inhibition in pickling baths is of great importance. The inhibition efficiency depends on the additive compounds, many factors which include the number of adsorption active centers and their charge density, molecular size and the mode of inter action with metal surface^[15] Weight loss determinations of aluminum in 0.5 M HCl after 30 min yielded convincing evidence for the application of H₂OAPA. The resulting quantity, corrosion rate, is thus a fundamental measurement in corrosion science^[16]. Corrosion rates can be evaluated by measuring either the concentration of the dissolved metal in solution by chemical analysis or by measuring weight of a specimen the corrosion behavior of a metal in aqueous environment is characterized.

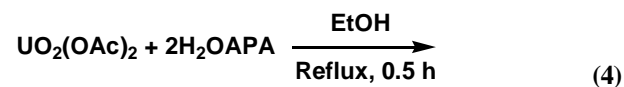
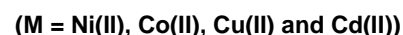
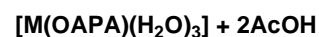
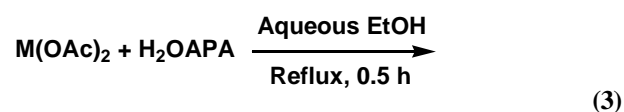
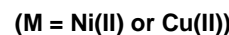
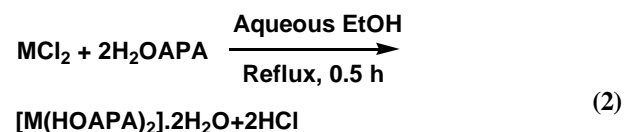
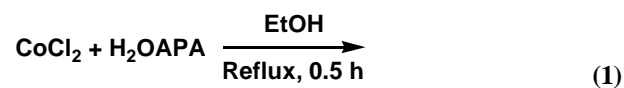
Biological activity

Antimicrobial activity. The ligand and some com-

plexes were tested as antibacterial agents at the department of microbiology, Faculty of Sciences, Mansoura university- seeded agar plates were prepared by putting 50 ml of inoculated agar into 15 cm petri-dishes and allowing them to solidify. Cups were made to receive 25ml of the solution and allowed to diffuse and incubate at 37° C for 24 h. inhibition zone was measured^[17] and compared with that of gentamicin solution (commercial antibiotic, Memphis Co., Egypt, 1000µg ml⁻¹). The experiment control was DMSO.

RESULTS AND DISCUSSION

The physical data of the complexes together with their elemental analyses and conductivities are listed in TABLE 1. The formation of complexes may be represented by the following equation.



The results indicates that all metal complexes are stable in air and insoluble in most organic solvent and most of them are completely soluble in dimethylformamide (DMF) and dimethylsulphoxide (DMSO). The molar conductivities (Λ_m) in DMSO at 25° C for all complexes are in the range (1-10) ohm⁻¹ cm² mol⁻¹, indicating their nonelectrolytic nature^[18].

IR and H¹NMR spectral studies

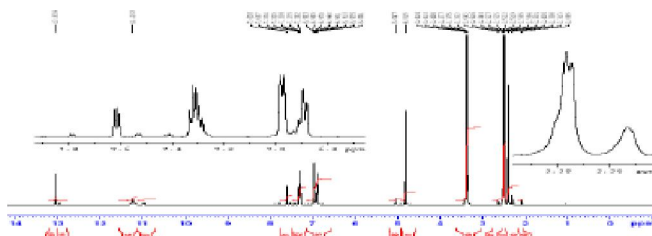
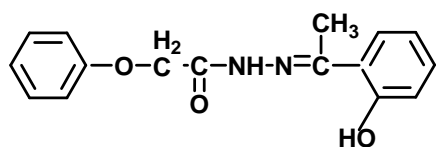
The IR Spectrum of H₂OAPA exhibits intense ab-

TABLE 1 : Analytical and physical data of H₂OAPA and its metal complexes.

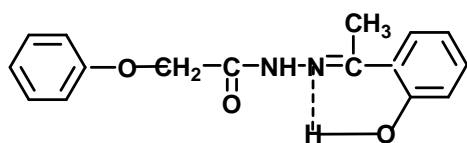
Compound	Empirical Formula	Yield %	Color	M.P. °C	% calc (found)				Λ_m^a in DMSO
					C	H	M	Cl ⁻	
H ₂ OAPA	C ₁₆ H ₁₆ N ₂ O ₃	87	Yellow	152	67.6 (67.2)	5.7 (5.5)	-	-	-
[Co(H ₂ OAPA)Cl ₂ (H ₂ O) ₂]	CoC ₁₆ H ₂₀ N ₂ O ₅ Cl ₂	85	Brike red	>300	42.7 (42.4)	4.5 (4.2)	13.1 (13.2)	15.8 (15.6)	8
[Cu(HOAPA) ₂].2H ₂ O	CuC ₃₂ H ₃₄ N ₄ O ₈	80	Yellowish Green	>300	57.7 (57.5)	5.1 (5.0)	9.5 (9.2)	-	2
[Ni(HOAPA) ₂].2H ₂ O	NiC ₃₂ H ₃₄ N ₄ O ₈	84	Green	>300	58.1 (58.2)	5.2 (5.1)	8.9 (8.6)	-	10
[UO ₂ (HOAPA) ₂]	UC ₃₂ H ₃₀ N ₄ O ₈	84	Red	>300	45.9 (45.0)	3.6 (3.3)	28.5 (28.2)	-	1
[Co(OAPA)(H ₂ O) ₃]	CoC ₁₆ H ₂₁ N ₂ O ₆	80	Brown	>300	48.5 (48.5)	5.3 (5.0)	14.9 (14.6)	-	6
[Ni(OAPA)(H ₂ O) ₃]	NiC ₁₆ H ₂₁ N ₂ O ₆	85	Green	>300	48.5 (48.3)	5.3 (5.1)	14.8 (14.7)	-	3
[Cu(OAPA)(H ₂ O) ₃]	CuC ₁₆ H ₂₁ N ₂ O ₆	82	Green	>300	47.9 (47.0)	5.3 (5.5)	15.8 (15.7)	-	2
[Cd(OAPA)(H ₂ O) ₃]	CdC ₁₆ H ₂₁ N ₂ O ₆	79	White	>300	42.7 (42.4)	4.7 (4.9)	25.0 (25.3)	-	1

 $(\Lambda_m) = \bar{U}^{-1} \text{ cm}^2 \text{ mol}^{-1}$ TABLE 2 : IR spectral data of H₂OAPA and its metal complexes.

Compound	$\nu(\text{C}=\text{O})$	$\nu(\text{C}=\text{N})$	$\nu(\text{C}=\text{N}-\text{N}=\text{C})$	$\nu(\text{C}-\text{O})$	$\nu(\text{C}-\text{O})_{\text{phenolic}}$	$\delta(\text{OH})$	$\nu(\text{N}-\text{N})$	$\nu(\text{M}-\text{O})$	$\nu(\text{M}-\text{N})$
H ₂ OAPA	1700	1615	-	-	1300	1152	1061	-	-
[Co(H ₂ OAPA)Cl ₂ (H ₂ O) ₂]	1655	1601	-	-	1297	1130	1081	525	420
[Cu(HOAPA) ₂].2H ₂ O	1635	1600	-	-	1330	-	1085	510	420
[Ni(HOAPA) ₂].2H ₂ O	1640	1596	-	-	1323	-	1087	520	420
[UO ₂ (HOAPA) ₂]	1634	1595	-	-	1312	-	1091	520	410
[Co(OAPA)(H ₂ O) ₃]	-	-	1592	1371	1340	-	1080	520	420
[Ni(OAPA)(H ₂ O) ₃]	-	-	1572	1375	1339	-	1080	523	420
[Cu(OAPA)(H ₂ O) ₃]	-	-	1595	1391	1340	-	1083	530	420
[Cd(OAPA)(H ₂ O) ₃]	-	-	1590	1390	1339	-	1080	511	410

Figure 1 : ¹H NMR Spectrum of H₂OAPA

Structure (I)



Structure (II)

sorption band at 1700 cm^{-1} due to $\nu(\text{C}=\text{O})$ ^[19]. The $\nu(\text{C}=\text{N})$ appears as a shoulder at 1615 cm^{-1} . The spectrum gives two bands at 3393 and 3130 cm^{-1} attributable to $\nu(\text{OH})$ and $\nu(\text{NH})$ ^[20], respectively. The medium intensity bands at 1300, 1152 and 1061 cm^{-1} are assigned to $\nu(\text{C}-\text{O})_{\text{phenolic}}$, $\delta(\text{OH})$ ^[21] and $\nu(\text{N}-\text{N})$ ^[22], respectively.

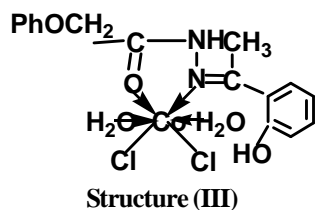
The ¹H NMR spectrum of H₂OAPA in DMSO-d₆ (Figure 1) shows multiplet signals in the δ 6.88- 7.62 ppm range assigned to the aromatic protons. The two signals at δ 13.06 and δ 11.23 ppm are attributable to the two protons of (OH) phenolic and (NH) group, respectively. The appearance of the signal due to the proton of (OH) phenolic at high value downfield from TMS suggest the presence of intramolecular hydrogen bonding between the phenolic oxygen (OH) and azomethine nitrogen (C=N) group as shown in (Struc-

Full Paper

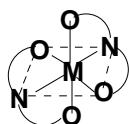
ture II). The sharp singlet observed at δ 2.64 ppm is assigned to the methyl protons ($-\text{N}=\text{C}-\text{CH}_3$).

A comparison of IR spectra of H_2OAPA and its metal complexes (TABLE 2) shows that H_2OAPA behaves as a neutral bidentate and a mononegative or bidentate tridentate ligand depending upon the metal salt used and the conditions of preparation as well as the pH of the medium.

The IR spectra of the $[\text{Co}(\text{H}_2\text{OAPA})\text{Cl}_2(\text{H}_2\text{O})_2]$ complex reveals that H_2OAPA behaves as a neutral bidentate ligand coordinating via the carbonyl oxygen ($\text{C}=\text{O}$) and the azomethine nitrogen ($\text{C}=\text{N}$) forming five member ring including the cobalt atom. This mode of coordination (Structure III) is supported by the following evidences: (i) $\nu(\text{C}=\text{N})$ and $\nu(\text{C}=\text{O})$ shift to lower wavenumber, (ii) $\nu(\text{N}-\text{N})$ shifts to higher wavenumber, (iii) $\nu(\text{C}-\text{O})$ phenolic remains unchanged, indicating that phenolic oxygen is not involved in bonding and (iv) the appearance of new bands at 525 and 420 cm^{-1} attributed to $\nu(\text{Co}-\text{O})$ ^[23] and $\nu(\text{Co}-\text{N})$ ^[24] respectively.



On the other hand, the IR spectra of $[\text{M}(\text{HOAPA})_2]_n(\text{H}_2\text{O})$ ($\text{M} = \text{Ni}(\text{II}), \text{Cu}(\text{II})$ and $\text{U}(\text{VI})\text{O}_2$; $n=0$ or 2) reflect that the ligand behaves as a mononegative tridentate ligand coordinating via the carbonyl oxygen ($\text{C}=\text{O}$), the azomethine nitrogen ($\text{C}=\text{N}$) and the deprotonated phenolic oxygen. This mode of complexation (Structure IV) is suggested on the basis of the following observations: (i) $\nu(\text{C}=\text{N})$ and $\nu(\text{C}=\text{O})$ shift to lower wavenumber (ii) $\nu(\text{N}-\text{N})$ and $\nu(\text{C}-\text{O})$ ^[25] phenolic shift to higher wavenumber, (iii) the disappearance of $\delta(\text{OH})$ and (iv) the appearance of new bands in the $510-520$ and $410-420\text{ cm}^{-1}$ regions assignable to $\nu(\text{M}-\text{O})$ ^[23] and $\nu(\text{M}-\text{N})$ ^[24], respectively.



($\text{M} = \text{Ni}(\text{II}), \text{Cu}(\text{II})$ and $\text{U}(\text{VI})\text{O}_2$; $n=0$ or 2)
Structure (IV)

In the ^1H NMR spectrum of $[\text{UO}_2(\text{HOAPA})_2]$ complex (Figure 2), the signals due to the OH protons disappears confirming deprotonation occurs through OH Phenolic group, while the signal due to NH proton undergoes a strong field shifting suggesting coordination of adjacent hydrazide $>\text{C}=\text{O}$ and $>\text{C}=\text{N}$ with the metal ion^[26].

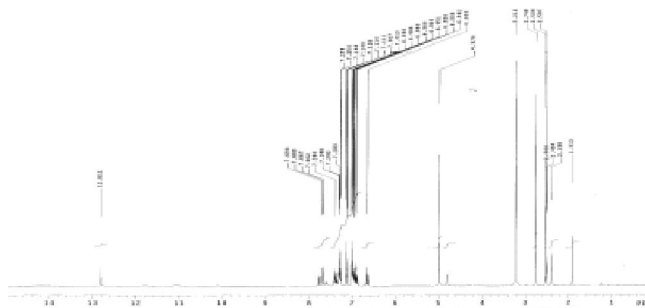
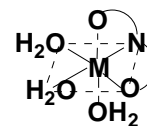


Figure 2 : ^1H NMR Spectrum of $[\text{UO}_2(\text{HOAPA})_2]$

Finally, the IR spectra of $[\text{M}(\text{OAPA})(\text{H}_3\text{O})_3]$, ($\text{M} = \text{Co}(\text{II}), \text{Ni}(\text{II}), \text{Cu}(\text{II})$ and $\text{Cd}(\text{II})$) show that H_2OAPA behaves as a bidentate tridentate ligand coordinating via the deprotonated phenolic oxygen, the deprotonated enolized carbonyl oxygen ($=\text{C}-\text{O}^-$) and the azomethine nitrogen ($\text{C}=\text{N}$). This mode of chelation (Structure V) is confirmed by the following evidences: (i) the disappearance of $\nu(\text{C}=\text{O})$ and $\delta(\text{OH})$ and $\nu(\text{C}=\text{N})$ with simultaneous appearance of new bands in the $1371-1391$ and $1573-1592\text{ cm}^{-1}$ regions assignable to $\nu(\text{C}-\text{O})$ and $\nu(\text{C}=\text{N}-\text{N}=\text{C})$ ^[6, 10], respectively, (ii) $\nu(\text{C}-\text{O})$ ^[27] phenolic and $\nu(\text{N}-\text{N})$ shift to higher wavenumber and (iii) the appearance of new bands in the $511-530$ and $410-420\text{ cm}^{-1}$ regions attributable to $\nu(\text{M}-\text{O})$ ^[23] and $\nu(\text{M}-\text{N})$ ^[24], respectively.



($\text{M} = \text{Co}(\text{II}), \text{Ni}(\text{II}), \text{Cu}(\text{II})$ and $\text{Cd}(\text{II})$).
Structure (V)

Strong evidence for the deprotonation of enolized carbonyl oxygen $=\text{C}-\text{OH}$ and the phenolic oxygen (OH) comes from the ^1H NMR spectrum of the diamagnetic $[\text{Cd}(\text{OAPA})(\text{H}_2\text{O})_3]$ complexes (Figure 3) which show the absence of the signals at δ 13.06 and δ 11.23 ppm assigned to the (OH) and (NH) protons, respectively.

The uranyl complex exhibits two bands at 925 and

Full Paper

The electronic spectra of $[\text{Cu}(\text{HOAPA})_2] \cdot 2\text{H}_2\text{O}$ (Figure 4) and $[\text{Cu}(\text{OAPA})(\text{H}_2\text{O})_3]$ give two absorption bands in the 14486 -15873 and 17241 -18087 cm^{-1} attributed to ${}^2\text{B}_{1g} \rightarrow {}^2\text{E}_g$ and ${}^2\text{B}_{1g} \rightarrow {}^2\text{A}_{1g}$ transition, in a tetragonally distorted octahedral configurations^[33,35]. The band in the 28571- 31250 cm^{-1} region may be assigned to Cu-L charge transfer^[29]. The magnetic moment values of Cu(II) complexes (2.01 – 2.2 B.M) lie with the range of Cu(II) ions in a d^9 system^[36].

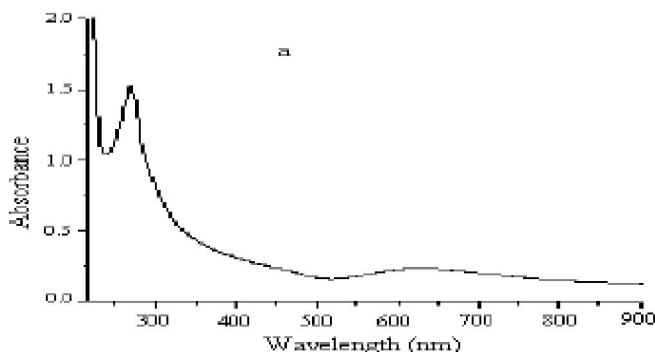


Figure 4 : Electronic spectra of: a- $[\text{Cu}(\text{HOAPA})_2] \cdot 2\text{H}_2\text{O}$

Finally, The UV spectrum of the $[\text{UO}_2(\text{HOAPA})_2]$ (Figure 5) complex shows two bands at 23809 and 29412 cm^{-1} assignable to ${}^1\Sigma_g^+ \rightarrow {}^2\Pi_u$ transition of dioxurium(VI) and charge transfer probably $n \rightarrow \pi^*$ transition, respectively^[37].

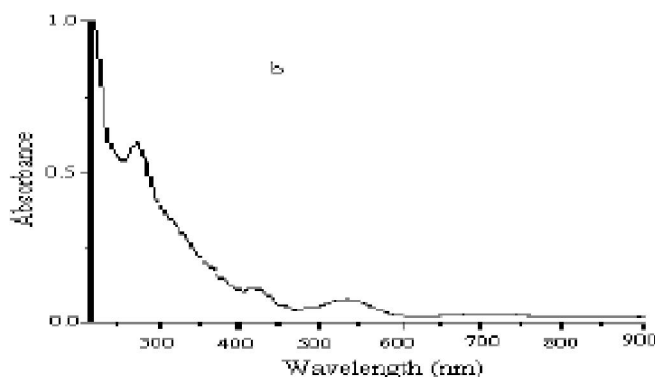


Figure 5 : Electronic spectra of: b- $[\text{UO}_2(\text{HOAPA})_2]$

Corrosion inhibition by the chemical technique

The linear variation of weight loss with time (Figure 6) in uninhibited and inhibited 0.5M hydrochloric acid indicated the absence of insoluble surface films during corrosion. In the absence of any surface film, the inhibitors are first adsorbed onto the metal surface and thereafter impede corrosion either by merely blocking the reaction sites (anodic and cathodic) or by altering the mechanism of the anodic and cathodic partial pro-

cesses. The percentage inhibition efficiency (% IE) of the investigated compounds (TABLE 4) was determined

using the equation $\% \text{IE} = \frac{\Delta W - \Delta W_i}{\Delta W} \times 100$. This means

that the presence of these compounds retards the corrosion. The decrease in corrosion rate of aluminum in 0.5M hydrochloric acid in the presence of these investigated compounds indicates that these compounds act as inhibitors.

TABLE 4 : (% Inhibition efficiency (%IE) at different concentrations of the investigated compounds for the corrosion of aluminum in 0.5 M HCL at 30°C).

Concentration M	H2OAPA (%IE)
5×10^{-5}	38.7
1×10^{-4}	58.2
5×10^{-4}	67.7
1×10^{-3}	87.1
5×10^{-3}	90.3

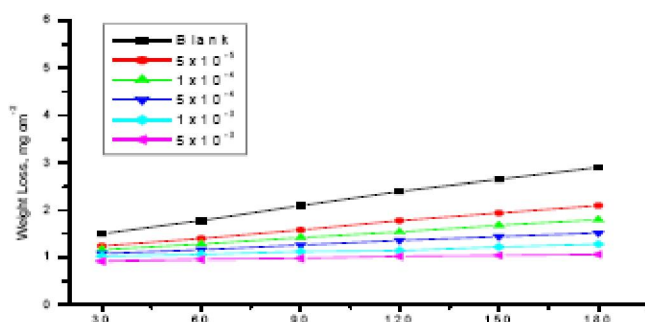


Figure 6 : Weight loss-time curves for the corrosion of aluminum in 0.5 M HCl in the absence and presences of different concentration of compound (H_2OAPA) at 30° C

TABLE 5 : Inhibition zones diameter (I.Z.D) in mm as a criterion of antibacterial activity of the ligande and some complexes at concentration level of 2 mg ml-1.

Compounds	Bacteria	
	Bacillus (G +ve)	Pseudomonas (G -ve)
	I.Z.D.(mm)	I.Z.D.(mm)
H_2OAPA	0	0
$[\text{Cu}(\text{OAPA})(\text{H}_2\text{O})_3]$	0	0
$[\text{Co}(\text{H}_2\text{OAPA})\text{Cl}_2(\text{H}_2\text{O})_2]$	21	0
$[\text{Co}(\text{OAPA})(\text{H}_2\text{O})_3]$	14	0
$[\text{Cd}(\text{OAPA})(\text{H}_2\text{O})_3]$	22	0
$[\text{UO}_2(\text{HOAPA})_2]$	0	0

Antimicrobial activity : The antimicrobial activity data for H_2OAPA and its metal complexes against *Bacillus thuringiensis* and *pseudomonas aureginosa* are

compiled in TABLE 5. Growth inhibition zones are proportional to the antimicrobial activity of the tested compound. The data suggest that cobalt (II) and cadmium (II) complexes were affected by the tested chemicals with strongest activity for Gram-Positive. On the other hand, H₂OAPA as well as its complexes do not show appreciable antimicrobial activity against the Gram-Negative bacteria.

REFERENCES

- [1] S.Sivaramaiah, P.R.Reddy; *J.Anal.Chem.*, **60**, 828 (2005).
- [2] S.H.Babu, K.Suvaradhan, K.S.Kumar, K.M.Reddy, D.Rekha, P.Chiranjeeui; *J.Hazand.Mater B.*, **120**, 213 (2005).
- [3] S.A.Berger; *J.Microchem.*, **47**, 317 (1993).
- [4] B.Singh, P.Srivastava; *Transition Met.Chem.*, **11**, 106 (1986).
- [5] M.S.Soliman, M.A.Khattab; *Bull.Soc.Chim.Fr.*, 894 (1991).
- [6] T.R.Rao, M.Sahay, R.C.Aggarwal; *Synth.React.Inorg.Met-Org.Chem.*, **15**, 175 (1985).
- [7] T.R.Rao, G.Singh; *Proc.Indian Acad.Sci.Chem.Sci.*, **101**, 219 (1989).
- [8] T.R.Rao, G.Singh; *Transition Met.Chem.*, **14**, 471 (1989).
- [9] M.M.Abou Sekkina, M.R.Salam; *Journal of Thermal analysis and Calorimetry.*, **48**, 841 (1997).
- [10] P.B.Sreeja, M.R.P.Kurup, A.Kishore, C.Jaswin; *Polyhedron.*, **23**, 575 (2004).
- [11] A.Syamal, M.R.Maurya; *Transition Met.Chem.*, **11**, 235 (1986).
- [12] K.M.Ibrahim; *Mans.Sci.Bull.*, **19**, 31 (1992).
- [13] A.A.El-Bindary; *Monatshete Fur.Chemie.*, **125**, 811 (1994).
- [14] K.K.Narang, R.A.Lal; *Transition Met.Chem.*, **3**, 272 (1978).
- [15] I.L.Rozenfeld; *Corrosion Inhibitors*, McGraw Hill, New York, (1981).
- [16] American Society for Testing and Materials, *Annual Book of ASTM Standards*, 10 (1980).
- [17] P.Gerhardt; *Manual of Methods for General Bacteriology*, American Society for Microbiology, Castello, (1981).
- [18] W.J.Geary; *Coord.Chem.Rev.*, **7**, 81 (1971).
- [19] S.Y.Chundak, V.M.Leovac, D.Z.Obadovic, D.M.Petrovic; *Transition Met.Chem.*, **11**, 308 (1986).
- [20] G.M.Abu El-Reash, M.M.Bekheit, K.M.Ibrahim; *Transition Met.Chem.*, **15**, 357 (1990).
- [21] N.Nawar, N.M.Hosney; *Chem.Pharm.Bull.*, **47**, 944 (1999).
- [22] T.H.Rakha; *Synth.React.Inorg.Met.-Org.Chem.*, **30**, 205 (2000).
- [23] A.N.Speca, N.M.Karyanis, L.L.Pytlewski; *Inorg.Chim.Acta.*, **9**, 87 (1974).
- [24] B.Becroft, M.J.M.Campbell, R.Grzeskowiak; *J.Inorg.Nucl.Chem.*, **36**, 55 (1974).
- [25] B.Singh, R.N.Singh, R.C.Aggarwal; *Polyhedron.*, **4**, 401 (1985).
- [26] T.R.Rao, G.Singh; *Transition Met.Chem.*, **14**, 471 (1989).
- [27] S.A.Patil, V.H.Kulkarni; *Inorg.Chim.Acta.*, **95**, 195 (1984).
- [28] A.T.T.Hsieh, R.M.Sheahan, B.O.West; *Aust.J.Chem.*, **28**, 885 (1975).
- [29] S.P.McGlynn, J.K.Smith; *J.Mol.Spectroscopy*, **6**, 164 (1961).
- [30] L.H.Jones; *Spectrochim.Acta.*, **15**, 409 (1959).
- [31] T.H.Rakha, N.Nawar, G.M.Abu El-Reash; *Synth.React.Inorg.Met-Org.Chem.*, **26**, 1705 (1996).
- [32] J.Lewis, R.G.Wilins; *Modern Coordination Chemistry*, Interscience., New York, (1960).
- [33] A.B.P.Lever; "Inorganic Electronic Spectroscopy", Elsevier, Amsterdam, (1984).
- [34] S.Singh, B.P.Yadva, R.C.Aggarwal; *Indian J.Chem.*, **23A**, 441 (1984).
- [35] L.Sacconi; *Transition Met.Chem.*, **4**, 199 (1979).
- [36] M.Palaniandavar, C.Natarajan; *Aust.J.Chem.*, **33**, 737 (1980).
- [37] R.G.Ghatlacharya, D.C.Bera; *J.Indian Chem.Soc.*, **52**, 373 (1975).